

Controllable Person Image Synthesis with Spatially-Adaptive Warped Normalization

JICHAO ZHANG, University of Trento
 ALIAKSANDR SIAROHIN, University of Trento
 HAO TANG, University of Trento
 JINGJING CHEN, Zhejiang University
 ENVER SANGINETO, University of Trento
 WEI WANG, University of Trento
 NICU SEBE, University of Trento



Fig. 1. Our controllable person image generation results: (a) pose transfer task; (b) texture transfer task.

Controllable person image generation aims to produce realistic human images with desirable attributes (e.g., the given pose, cloth textures or hair style). However, the large spatial misalignment between the source and target images makes the standard architectures for image-to-image translation not suitable for this task. Most of the state-of-the-art architectures avoid the alignment step during the generation, which causes many artifacts, especially for person images with complex textures. To solve this problem, we introduce a novel Spatially-Adaptive Warped Normalization (SAWN), which integrates a learned flow-field to warp modulation parameters. This allows us to align person spatial-adaptive styles with pose features efficiently. Moreover, we propose a novel self-training part replacement strategy to refine the pretrained model for the texture-transfer task, significantly improving the quality of the generated cloth and the preservation ability of irrelevant regions. Our experimental results on the widely used DeepFashion dataset demonstrate a significant improvement of the proposed method over the state-of-the-art methods on both pose-transfer and texture-transfer tasks.

Authors' addresses: Jichao Zhang, University of Trento, jichao.zhang@unitn.it; Aliaksandr Siarohin, University of Trento, aliaksandr.siarohin@unitn.it; Hao Tang, University of Trento, hao.tang@unitn.it; Jingjing Chen, Zhejiang University, jingjingchen@zju.edu.cn; Enver Sangineto, University of Trento, enver.sangineto@unitn.it; Wei Wang, University of Trento, wei.wang@unitn.it; Nicu Sebe, University of Trento, sebe@disi.unitn.it.

CCS Concepts: • **Computing methodologies** → **Texturing**; *Computer vision*.

Additional Key Words and Phrases: Neural Rendering, Generative Models, Controllable Person Image Generation

1 INTRODUCTION

In recent years, Generative Adversarial Networks (GANs) have shown a significant improvement in synthesizing realistic images [6, 26, 27] given a large amount of training data. Moreover, GANs opened the door to many creative applications, such as image translation [7, 67], image inpainting and editing [22, 41, 65], image animation [59, 66], including person image generation. Person image generation attracted a lot of attention in computer graphics and computer vision, due to its usefulness in data augmentation for surveillance [42], fashion design [15] and virtual try-on [13]. Compared to other common image types, a human image has rich variations in poses, clothing, hair styles, body shape, self-occlusions and other factors. Because of this, it is not easy to synthesize human images in a new target pose or wearing a new cloth without a 3D textured model for this specific person as supervision. Initial progress

has been made in the pose-guided person image generation task or pose-transfer for short. In the pose-transfer task, we are given a source image and a target pose and we are asked to generate a person from the source image in the target pose. The pose guided person image generation task was proposed by [33] and some improved models have been proposed [48, 51, 69]. Most of them follow a GAN architecture with an autoencoder-like generator which takes as input the target pose, usually represented by keypoints, and the person appearance, represented by an RGB image.

Recently, ADGAN [35] proposes an architecture for controllable person image generation which can be regarded as a generalization of the pose-guided person image generation. ADGAN [35] is not only able to perform the pose-transfer task, but also allows to transfer a texture of a particular person region while preserving the style of the irrelevant person regions. In more detail, given the source and reference images and the mask of a particular region, texture-transfer aims to copy the texture of the given segment from the reference image to the source image (see Fig. 1). Specifically, ADGAN is based on the ‘semantic image synthesis architecture’ [56], which learns to map a skeleton pose to an image by means of the style encoder that transfers the person style into pose features with the help of Adaptive Instance Normalization (AdaIN) [19].

However, as shown in Fig. 2 (3rd column), ADGAN tends to synthesize very blurry textures which lack the details. We argue that ADGAN learns the style parameters for AdaIN with multi-layer perceptrons, which neglects the spatial information of styles in person appearance. For example, given a person image, the body skin, garment, and hair styles should have different style features, and even the style is spatially-adaptive for different local regions of the garment. Thus, some researches have proposed the spatially-adaptive normalization which learns style parameter with spatial information for semantic image editing tasks [38, 68]. However, the spatially-adaptive instance normalization directly used in person image generation would lead to the spatial misalignment problem in the feature space between style parameters and pose features. In more details, the previous methods [25, 35] learn the mapping from the target pose to the target appearance by using the source appearance as the style input, which encounters the feature misalignment problem between the target pose and the source style. Recently, PISE [25] proposes a spatially-aware normalization and uses VGG features to constrain pose and style features in the same domain. However, we observe that PISE also fails in generating and transferring complex textures (Fig. 2 (4th column)), as its constraint is very weak and lacks an explicitly spatial warping operation to align style parameters and pose features.

To solve this problem, we propose a novel spatially-adaptive warped normalization (SAWN) which takes the learned flow-field as the condition to warp the scales and bias of modulation in the normalization to align the style features with the pose features. This operation is applied for multiple scales of the decoder. Additionally, we propose a self-training part replacement strategy to refine the trained model, which could further improve the quality of the generated samples and preserve the consistency of other regions. In more detail, we finetune the network by performing texture-transfer task by person part replacement operation between the same person



Fig. 2. Comparison of texture transfer on clothes between our method and the baselines: ADGAN [35] and PISE [25]. The 1st row shows that our model achieves better complex texture transfer (labelled with green box), and the 2nd row shows that our model better preserves irrelevant regions (labelled with the blue box).

in different poses. This two modifications bring a significant improvement to the quality of the generated textures (see Fig. 2 (5th column)).

In summary, the main contributions of this work are:

- 1) We propose a novel spatially-adaptive warped normalization which integrates the learned flow field to warp the scales and bias parameters to align the style and pose features.
- 2) We propose a novel training strategy, i.e., the self-training part replacement to refine the trained model, which reduces the discrepancy between the training and test phases, and further improve the quality of texture-transfer results and attain better preservation of some regions.
- 3) Our model achieves state-of-the-art pose-guided person image generation results and outperforms all existing methods in the texture-transfer task, especially for complex textures.

2 RELATED WORK

Pose-Guided Person Image Generation. In the short span of five years, generative adversarial networks (GANs) [10] opened the door to many creative applications and have come to dominate the field of image inpainting [22], image editing [2, 41, 65], 2D and 3D image synthesis [1, 3, 7, 13, 20, 36, 39, 52, 63, 67] and person image generation. Most of the models for person image generation are based on GANs and can be divided into two groups depending on the underlined target pose representation, i.e., 2D keypoints or SMPL [32] correspondences which are estimated using DensePose [12].

The first group of approaches [5, 17, 30, 33, 34, 50, 51] exploit keypoints encoded as heatmaps. This approach was initially proposed by PG2 [33]. Specifically, PG2 [33] consists of two key stages: first, a U-Net is used to generate a coarse person image with a target pose, then another U-net is used to refine the image generated previously. However, the photorealistic person generation with accurate preservation of complicated textures is beyond the reach of this model, as this model struggles to handle large spatial variations and non-rigid deformation between different poses. Then, a set of studies explored ways to handle the deformation between different poses [44, 48, 69].

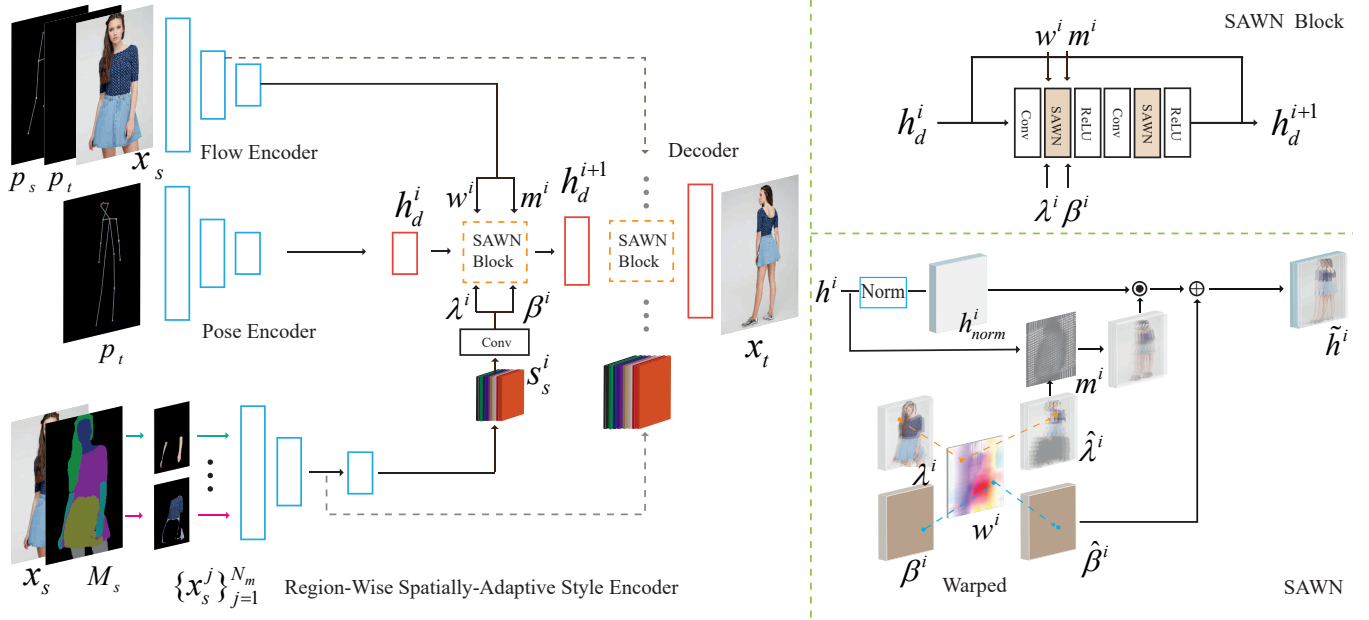


Fig. 3. The overview of our architecture with the proposed spatially-adaptive warped normalization (SAWN). Our architecture consists of one flow encoder, a pose encoder, a region-wise spatially-adaptive style encoder and one decoder integrating with our SAWN block at multiple scales. Our style encoder attains multi-scale style features $\{s_s^i\}_{i=1}^{N_s}$ where the corresponding channels for style features s_s^i are attained from the encoder blocks by taking person parts x_s^j as input. h^i represents the features before normalization.

For instance, Siarohin et al. [48] propose a deformable skip connection for the generator which ‘move’ local information according to the structural deformations from different poses. However, this method requires the pre-defined transformation components, which limits its applications. Zhu et al. [69] propose progressive attention transfer blocks (PATBs) in feature level which could focus on the local transfer in the manifold, therefore circumventing the difficulty of capturing the pose variation in the global structure. Then, Tang et al. [51] optimize the PATBs module of Pose-Attn [69] with a mutually learning module between appearance and pose. However, both methods still struggle to generate photorealistic person images with accurate preservation of the complex textures, as these methods do not explicitly learn the spatial transformation between different poses. Recently, Ren et al. [44] propose a GFLA module to explicitly warp the features with the learned flow field. Additionally, their local-attention module avoids the poor gradient propagation of the bilinear sampling. Compared with the previous methods, GFLA achieves high-quality results, but excessive freedom in feature warping leads to erroneous preservation of the global identity information. Additionally, GFLA cannot perform texture-transfer tasks, as it lacks the disentangled module for appearance.

The second group of approaches is based on the rich 3D SMPL [32] correspondences as pose presentation. For instance, Neverova et al. [37] use DensPose to guide the proposed predictive module and the warping module. The warping module aims to warp the texture to the UV coordinates and performs the inpainting for UV texture, then warps back to the target image. At the same time, the predictive module is a generative model conditioned on the DensePose. The results from the two modules are passed into the blending module to attain more realistic results. Rather than working directly with

the RGB texture for inpainting, Grigorev et al. [11] predict the coordinates of the texture elements in the input UV-space and extract the colors from the source images to generate the final textures. Finally, Kripasindhu et al. [47] employ a learned high-dimensional UV feature map to encode the appearance using the inpainting module. Then, the UV feature map is rendered in the desired target pose and is passed through a translation network that creates the final rendered image. However, the results of these methods have visual artifacts as it is difficult for the inpainting model to construct the precise UV texture since it has no UV ground truth for training.

In this paper, we exploit keypoints instead of SMPL.

Person Texture-Transfer. This task aims to produce realistic person images where the texture of one or several person regions is inherited from the reference image, while other person regions remain intact. Men et al. [35] propose a novel architecture (ADGAN) for this task, and their model regards the pose as content, person image as style, and transfers the style code into the target pose by using a style module based on adaptive instance normalization [19]. Other works [68, 70] are based on the general semantic image synthesis model and can be used to implement the manipulation of the person attributes. However, a large spatial misalignment between the source segmentation and target garments is not taken into account which causes low-quality generation for images with large pose variations and complex textures. Recently, PISE [25] presented a spatially-aware normalization and used the VGG feature to put the pose and style features into the same feature space. However, PISE also fails in generating and transferring complex texture, as it lacks an explicit spatial warped operation to align pose and style features. Concurrent with our work, Sarkar et al. [46] propose a StyleGAN-based method that exploits SMPL [32] correspondences

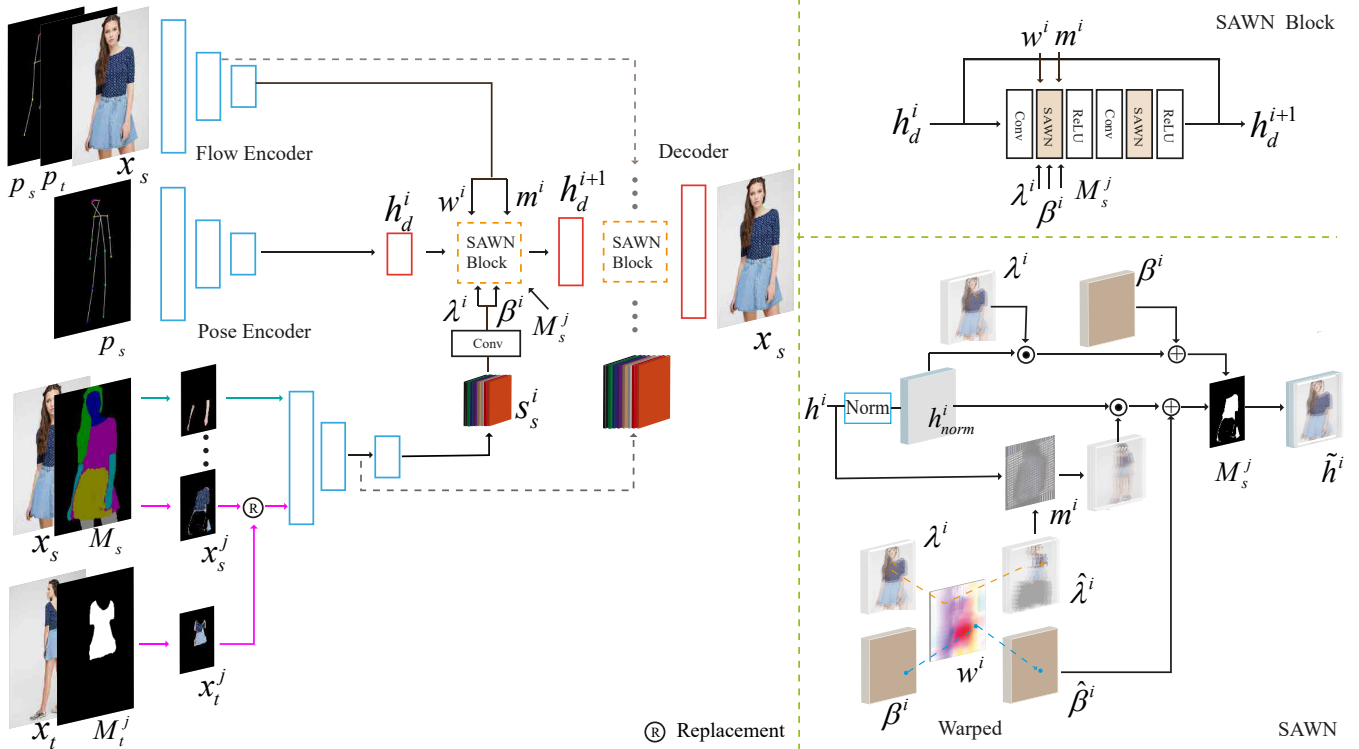


Fig. 4. The overview of our proposed Self-Training Part Replacement architecture. This architecture takes the source appearance x_s as input of the style encoder and the source pose p_s as the input of the pose encoder to reconstruct x_s . We randomly replace one part x_s^j using x_t^j from the target person x_t to attain mixed styles. Additionally, the mask M_s^j , indicating the replacement part is an input of our SAWN module for performing alpha blending.

as pose presentation and their model achieves high-quality generation and garment transfer results. Compared with it, our model does not exploit this 3D representation information to guide the generation.

Additionally, the person texture-transfer generation task is very similar to the virtual try-on task, which transfers a desirable clothing item onto the corresponding person [14, 24, 43, 55, 61, 62]. We argue that the differences lie in two aspects. First, our task in this paper is to edit multiple person regions, in addition to the garment. Second, in this task, we transfer the complex textures into the garment of the source person while we preserve the shape of the garment in this source person.

Conditional Normalization has been widely used for various vision tasks, such as style transfer [18], image translation [8, 21, 29, 38, 68], super-resolution [57] or random image generation [26]. Differently from previous unconditional normalization techniques [23, 53, 60], conditional normalizations [9, 18] requires external data which are used to infer the modulation parameters. Then, normalized activations are modulated by the scales and bias parameters previously inferred. Based on the adaptive instance normalization (AdaIN) [18], Taesung et al [38] propose a spatially-adaptive normalization which can effectively propagate the semantic information through the network while preserving the spatial information of the semantic representation. Some variations based on the spatially-adaptive normalization include conditional group normalization by using GroupNet instead of ConvNet [70], semantic region-adaptive normalization [68] with both style and mask inputs for regional

image editing, and class-adaptive normalization [49] which is only applicable to semantic class.

Compared with these previous methods, we integrate the learned flow field into adaptive instance normalization, which aims to warp the modulation parameters to align pose and style features.

3 PRELIMINARIES

Since our method is based on the spatially-invariant adaptive instance normalization [19, 26, 35] and the spatially-adaptive normalization [39], we first introduce the key ideas of these two approaches.

Spatially-Invariant Adaptive Instance Normalization. Spatially-Invariant Adaptive Instance Normalization (AdaIN) was initially introduced for style-transfer task [19]. Let $h^i \in B \times C^i \times H^i \times W^i$, where B , C^i , H^i and W^i represent batch size, number of channels, height and width respectively, denote the activations of the i -th layer in decoder. Spatially-invariant adaptive instance normalization can be generally formulated as:

$$\tilde{h}_{b,c,y,x}^i = \lambda_{b,c}^i \frac{h_{b,c,y,x}^i - \mu_{b,c}^i}{\sigma_{b,c}^i} + \beta_{b,c}^i, \quad (1)$$

where $\tilde{h}_{b,c,y,x}^i$ is the normalized value at index (b, c, y, x) , where $b \in [0, B-1]$, $c \in [0, C^i-1]$, $y \in [0, H^i-1]$, $x \in [0, W^i-1]$ and $\lambda^i \in R^{B \times C^i}$ and $\beta^i \in R^{B \times C^i}$ are the learned scale and bias. Usually both scale and bias are inferred by a multi-layer perceptron. Finally, μ^i and σ^i are

the mean and standard deviation of the input activations h^i which can be computed as:

$$\begin{aligned}\mu_{b,c}^i &= \frac{1}{H^i W^i} \sum_{y,x} h_{b,c,y,x}^i, \\ \sigma_{b,c}^i &= \sqrt{\frac{1}{H^i W^i} \sum_{y,x} ((h_{b,c,y,x}^i)^2 - (\mu_{b,c}^i)^2)}.\end{aligned}\quad (2)$$

To this end, both modulation parameters λ and β and normalization parameters σ and μ are the same across spatial coordinates.

Spatially-Adaptive Instance Normalization. As mentioned above, the previous baseline ADGAN uses the global style description provided by AdaIN and neglects the spatial information of the person image, which leads to unrealistic texture transfer. Thus, the modulation parameters λ^i and β^i should be spatially-adaptive, which means that they have the same spatial dimension as the input activations h^i . Spatially-adaptive instance normalization can be defined as:

$$\tilde{h}_{b,c,y,x}^i = \lambda_{b,c,y,x}^i \frac{h_{b,c,y,x}^i - \mu_{b,c}^i}{\sigma_{b,c}^i} + \beta_{b,c,y,x}^i. \quad (3)$$

4 METHOD

As shown in Fig. 3, our architecture consists of a flow encoder, a pose encoder, a style encoder, and a decoder with spatially-adaptive warped normalization (SAWN) module. The pose encoder takes the target pose p_t as input and extracts the pose features. The flow encoder takes the source pose p_s , the target pose p_t and the source person image x_s as input and output multi-scale flow fields $\{w^i\}_{i=1}^{N_s}$ (N_s is the number of scales) and occlusion masks $\{m^i\}_{i=1}^{N_s}$. The style encoder takes the source person x_s and the corresponding semantic segmentation M_s to extract region-aware style codes s_s^i in multiple scales, and then predicts the modulation parameters λ^i and β^i using a single conv-block. The decoder consists of several SAWN blocks taking the learned flow field w^i , occlusion mask m^i , modulation parameters λ^i , β^i and previous layer features h_d^i as inputs and generating a new feature h^{i+1} . This process is repeated at each scale i . Finally the decoder produces the output image \tilde{x}_t . The SAWN block aims to align the style features with pose features by warping the modulation parameters. Later the warped parameters are used to modulate the normalized features. Our SAWN extends the spatially-adaptive instance normalization presented in Section 3 and the details are introduced below.

Spatially-Adaptive Warped Normalization. Based on the spatially-adaptive instance normalization, we propose a spatially-adaptive warped normalization (SAWN) to align the modulation parameters λ^i and β^i with the target pose feature and then modulate the normalized pose feature using the warped parameters. As shown in the bottom-right of Fig. 3, SAWN takes the feature h^i and other four parameters as inputs: scale λ^i , bias β^i , learned flow-field w^i and occlusion mask m^i .

In detail, first we normalize features h^i to attain normalized features h_{norm}^i . Then, we employ the flow-field w^i (two channels) to warp λ^i and β^i to attain warped parameters $\hat{\lambda}^i$ and $\hat{\beta}^i$ by means of

a bilinear sampling:

$$\begin{aligned}\hat{\lambda}^i(b, c, y, x) &= \lambda^i \left[b; c; y + w_{b,1,y,x}^i; x + w_{b,2,y,x}^i \right], \\ \hat{\beta}^i(b, c, y, x) &= \beta^i \left[b; c; y + w_{b,1,y,x}^i; x + w_{b,2,y,x}^i \right],\end{aligned}\quad (4)$$

where the square brackets represent the bilinear interpolation. Since the style parameter λ^i inferred from the source appearance does not provide all the content of the target appearance, due to the frequent self-occlusion, we perform an alpha blending between the scale $\hat{\lambda}^i$ and input activations h^i using the occlusion mask m^i . Our SAWN can be defined as:

$$\tilde{h}^i = ((\hat{\lambda}^i \odot m^i + h^i \odot (1 - m^i)) \odot h_{norm}^i \oplus \hat{\beta}^i). \quad (5)$$

As shown in Fig. 3, we use SAWN in every scale of the decoder. We tested several blending combinations and found that blending h^i and $\hat{\lambda}^i$ performs best. Additionally, we do not perform the blending for the parameter $\hat{\beta}^i$, as the style information is predominantly provided by the scale and not by the bias [27].

Region-Wise Spatially-Adaptive Encoder. To perform texture-transfer guided by the reference person region, we employ semantic segmentation to disentangle person attributes, such as garment and hair. As shown in the bottom-left of Fig. 3, we obtain the person parts $\{x_s^j\}_{j=1}^{N_m}$ (N_m is the number of the segmentation labels) by using the corresponding segmentation mask M_s^j multiplied with the person image x_s . Then, each part of $\{x_s^j\}_{j=1}^{N_m}$ is used as input of the style encoder to obtain the corresponding style codes. Finally, the style codes for all parts are concatenated into s_s^i , which is later processed by a single conv-block to produce the spatially-adaptive modulation parameters λ^i and β^i . Since the style codes are separately extracted from each person part and then concatenated, the input of the conv-block is disentangled with respect to the specific person regions, and this facilitates replacing the individual parts of the source person with the corresponding target parts. We refer to our style encoder as the region-wise spatially-adaptive style encoder.

Self-Training Part Replacement Strategy. The previous texture-transfer methods [25, 35] are usually trained in the same way as pose-guided generation methods, and at a test time the style code of the source person region is replaced with the reference person region. Since the model never observed such mixed style codes from different images at the train time, this causes a substantial quality degradation and bad texture preservation in the generated images. As shown in the Fig. 4, we propose a self-training part replacement architecture that integrates the part replacement operation by a self-training strategy.

In detail, we use the same training data as the architecture of Fig. 3, but there are two important differences. First, we use the source pose p_s and person x_s to reconstruct x_s instead of target person x_t , and we will randomly replace one part x_s^j of the source person x_s using part x_t^j from the target person x_t to produce mixed style codes in our style encoder. Second, we propose to use the segmentation mask M_s^j from M_s as an additional input of the SAWN block, which indicates the part that needs to be replaced. Note that M_s^j is used to perform local warped modulation and to preserve

other regions. Additionally, we use the same flow encoder with the architecture of Fig. 3.

As shown in bottom-right of Fig. 4, we can define the new SAWN with M_s^j as:

$$\begin{aligned}\tilde{h}_{warp}^i &= ((\lambda^i \odot m^i + h^i \odot (1 - m^i)) \odot h_{norm}^i \oplus \beta^i, \\ \tilde{h}_{nowarp}^i &= (\lambda^i \odot h_{norm}^i) \oplus \beta^i, \\ \tilde{h}^i &= \tilde{h}_{warp}^i \odot M_s^j + \tilde{h}_{nowarp}^i \odot (1 - M_s^j),\end{aligned}\quad (6)$$

where \tilde{h}_{warp}^i and \tilde{h}_{nowarp}^i indicate the modulation features obtained using warped parameters and obtained without warped parameters.

Training Losses. Similar to the previous baselines [25, 35], we employ four losses: adversarial loss ℓ_{adv} , L1 reconstruction loss ℓ_{recon} , VGG style loss ℓ_{ogg_s} , and VGG content loss ℓ_{ogg_c} for training both models. The overall loss is defined as:

$$\ell_{all} = \lambda_1 \ell_{adv} + \lambda_2 \ell_{recon} + \lambda_3 \ell_{ogg_s} + \lambda_4 \ell_{ogg_c}, \quad (7)$$

where $\lambda_1, \lambda_2, \lambda_3$ and λ_4 are hyper-parameters controlling the contribution of each loss term. Additionally, our discriminator just takes fake or real person images as input and does not use any other conditional information.

How to Perform Both Tasks in the Test Phase? We employ the model of Fig. 3 for pose-transfer (pose-guided person image generation) task (see Section 5.4.1). For the texture-transfer, on the other hand, we employ the model of Fig. 4, but use the person with a different identity as the reference image to produce results with the desired person attributes (see Section 5.4.2).

5 EXPERIMENTS

5.1 Dataset

We evaluate our model on the DeepFashion [31] (in-shop clothes retrieval benchmark) dataset, which is widely used in person image generation tasks. DeepFashion contains 52,712 person images with various poses and appearances, and each image has a resolution of 176×256. We resize all the images into 256×256 for both training and testing. We split the dataset following ADGAN [35], other state-of-the-art methods also adopt the same data configuration. In more detail, 101,966 pairs are randomly selected for training and 8,570 for testing. Additionally, we use the same segmentation masks for person images as ADGAN, obtained from the human parser [4]. For the evaluation of the texture transfer task, we sample 8,570 pairs with different identity from the test dataset, and select ‘Pants’, ‘Hair’, ‘Face’, ‘Tops’ regions for each pair.

5.2 Implementation Details

We follow the GFLA [44] to pretrain the flow encoder with the sampling correction loss to constrain the flow field to sample semantically similar regions and the regularization loss to force warping in local region to behave similar to affine transformation. More details can be found in the GFLA [44]. We set $\lambda_1=2.0$, $\lambda_2=5.0$, $\lambda_3=0.5$, and $\lambda_4=0.0025$. Additionally, we use the Instance Normalization [54] for the layers in both discriminator and generator. We use the ADAM [28] optimizer with $\beta_1=0.5$, $\beta_2=0.999$, and learning rate 0.0001 for training our model. All of the experiments are conducted on two 16GB Tesla V100 GPUs with the PyTorch framework [40].

Table 1. Quantitative results between ours with state-of-the-art methods on DeepFashion. GFLA (256) indicates the original GFLA [44] which is trained with 256×256 deepfashion images (resized from 1101×750). While we take the images resized from 256×176 to 256×256 as the inputs of GFLA for fair comparison.

Method	FID↓	LPIPS↓	User Study↑
Pose-Attn [69]	20.739	0.253	6.11%
XingGAN [51]	39.233	0.282	1.12%
GFLA (256) [44]	10.573	0.234	-
GFLA [44]	15.573	0.232	13.35%
BiGraph [50]	21.010	0.234	5.42%
ADGAN [35]	16.000	0.224	20.18%
PISE [25]	13.610	0.205	21.70%
Ours	11.540	0.196	32.12%

5.3 Evaluation Metrics

The selection of metrics to evaluate the quality of the generated images remains an open problem. The previous methods [33, 35, 48, 51, 69] exploit Inception score (IS) [45] as a metric to evaluate the quality of the generated samples and SSIM [58] as a metric to evaluate the similarity between the generated samples and the ground truth. However, recent works have verified that Fréchet Inception Distance (FID) [16] and Learned Perceptual Image Patch Similarity (LPIPS) [64] are more correlated with human evaluation than IS and SSIM. Thus, we follow GFLA [44] and utilize FID and LPIPS to evaluate all the models for pose-transfer. For the evaluation of texture-transfer we employ FID to measure the realism of the generated images, moreover, we adopt LPIPS to evaluate the consistency of the person regions that should not be transferred, which can be obtained by the corresponding mask. We refer to LPIPS for these regions as Mask-LPIPS. Lastly, we conduct user studies to assess the subjective quality and ask volunteers to select the most realistic image from both ground truth and generated images. Specifically, 20 volunteers were asked to choose the most realistic synthesized image from all models. Each of them was asked 50 questions.

5.4 State-of-the-Art Comparisons

We evaluate our model on two tasks, i.e., pose-transfer (pose-guided image generation) and texture-transfer. For a fair comparison, we compare our model with the state-of-the-art methods conditioned on 2D keypoints. Then, we conduct ablation studies to evaluate the effectiveness of the proposed SAWN and self-training part replacement strategy.

5.4.1 Pose-Transfer. The qualitative comparisons with state-of-the-art methods are shown in Fig. 5. We can observe that XingGAN [51], Pose-Attn [69] and ADGAN [35] have serious mode collapse appearance problems. GFLA [44] and PISE [25] on the other hand, suffer from serious appearance inconsistencies when generation assumes large spatial deformation. In contrast, our model could achieve sharper results with better appearance consistency, especially for complex texture transfer, for example, blue and black dress

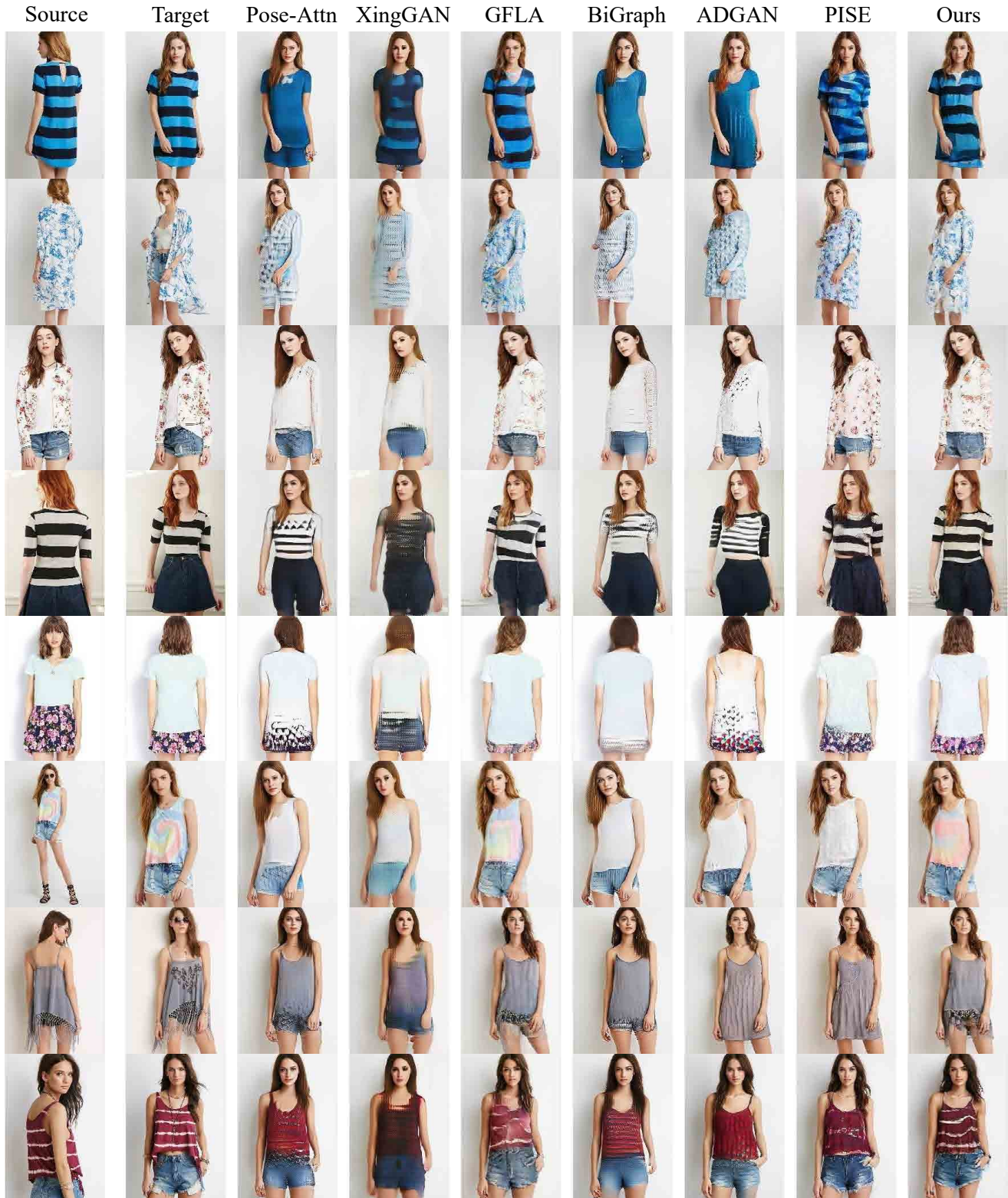


Fig. 5. Qualitative comparison between our method and the state-of-the-art methods, i.e., Pose-Attn [69], XingGAN [51], GFLA [44], BiGraph [50], ADGAN [35], and PISE [25] on the DeepFashion dataset.

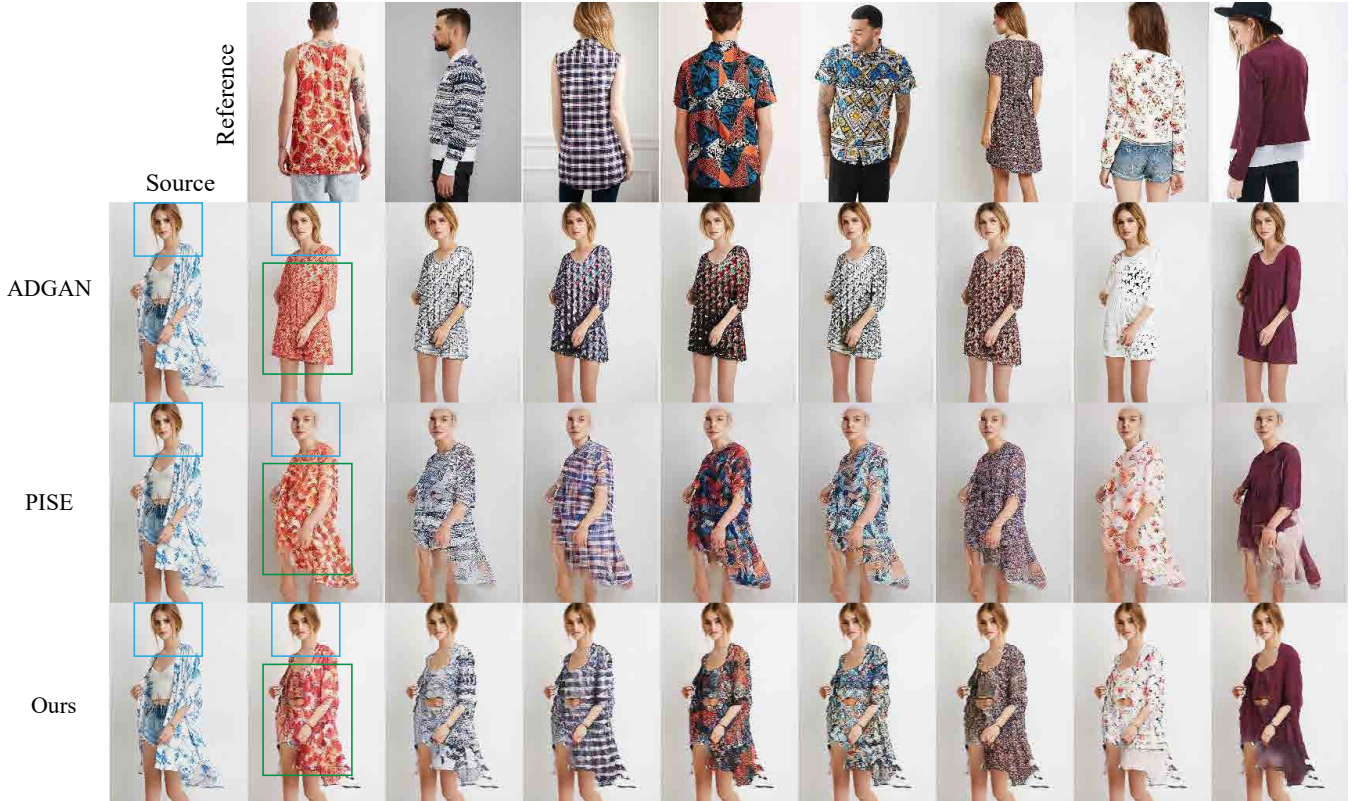


Fig. 6. Qualitative comparison of texture transfer between our method, ADGAN [35], and PISE [25]. Blue box: comparison of irrelevant attribute preservation. Green Box: comparison of garment texture transfer.

in the 1st row. The quantitative results are shown in Table 1, and it quantifies the improvement of our model in this task. In more detail, our model outperforms other methods on both metrics FID and LPIPS, which demonstrates that our results are more realistic and have better consistency in appearance and pose. Moreover, the user studies show that our model generates the most realistic results. More results and comparisons can be found in our demo video.

5.4.2 Texture-Transfer. We provide texture-transfer results guided by different reference person regions in Fig. 6. We show the comparisons between our results and the two leading methods for the texture-transfer in garments. It can be observed that our model achieves more realistic texture transfer (see green box). Given different reference persons with complex textures in garments, our model can render this texture into the garment region of the source image while preserving other regions, such as face and hair (see blue box). Moreover, ADGAN suffers from mode collapse in texture generation and fails to generate sharp images. Meanwhile, PISE achieves sharper results than ADGAN but worse than our model. Moreover, it is hard for PISE to preserve other regions such as the face and hair.

Moreover, we show more region transfer results, such as pants, hair style in Fig. 7. We arrive at a similar conclusion when comparing ours with both ADGAN and PISE. Specifically, ADGAN produces very blurry textures with missing original features ‘Pants’ region, comparing with both the 2nd and 3rd column results. PISE also fails

in preserving the other regions, such as face identity and sweater texture in Fig. 7(b).

Quantitative results have been shown in Table 2. Our model attains better FID and LPIPS scores in both ‘Pants’ and ‘Tops’ regions, and achieves better FID scores in all semantic regions, which indicates our model not only generates more realistic person images but also preserves better consistency of irrelevant attributes for ‘Pants’ and ‘Tops’ transfer tasks.

Overall, the qualitative and quantitative comparisons validate the effectiveness and superiority of our method on pose-transfer (pose-guided person image generation) and texture-transfer tasks. More results and comparisons can be found in our demo video.

5.5 Ablation Study

We conducted ablation studies to demonstrate the effectiveness of our proposed SAWN and self-training part replacement strategy, which we referred to as STPR.

Effect of SAWN. As shown in Fig. 8(a), we present the comparison between our full model with SAWN and our model with SAN (spatial-adaptive normalization without warping) instead of SAWN. We observe that our full model achieves sharper results and can transfer the complex texture from the source image into the target pose. Specifically, the first row of Fig. 8(a) shows that the full model could transfer the red-and-white textures into the target, while the variant with SAN could not. This validates the effectiveness of our



Fig. 7. More qualitative comparison of texture transfer between our method (4th row), ADGAN (2nd row) [35], and PISE (3rd row) [25]. (a, b, c) represent skirt, pants, and hair transfer, respectively.

Table 2. Quantitative results between our ours with state-of-the-art methods on DeepFashion.

Method	Pants		Hair		Face		Tops	
	FID↓	Mask-PIPS↓	FID↓	Mask-LPIPS↑	FID↓	Mask-LPIPS↓	FID↑	Mask-LPIPS↑
ADGAN [35]	14.80	0.057	15.23	0.061	15.35	0.049	14.37	0.195
PISE [25]	18.95	0.056	18.84	0.057	18.99	0.050	18.55	0.190
Ours	10.50	0.055	11.32	0.061	10.96	0.060	11.92	0.056

Table 3. Quantitative results between our full model and this model without STPR. STPR: self-training part replacement strategy.

Method	Pants		Hair		Face		Tops	
	FID↓	Mask-PIPS↓	FID↓	Mask-LPIPS↑	FID↓	Mask-LPIPS↓	FID↑	Mask-LPIPS↑
w/o STPR	12.13	0.056	13.00	0.061	12.13	0.056	15.72	0.057
Our full model	10.50	0.055	11.32	0.061	10.96	0.061	11.92	0.056

warped operation to align the features. As depicted in Table 4, our full model outperforms the variant with SAN on both LPIPS and FID metrics, which further demonstrates the effectiveness of our proposed SAWN.

Moreover, we visualize the learned flow fields and occlusion masks in Fig. 9. We apply the learned flow fields (2nd column) to directly warp input person (1st column) and obtain the warped results in pixel level (3rd column). It can be observed that the warped results in the pixel level have a very similar shape and appearance as the generated results (5th column) and target person (6th column), which further validates the ability of our model to learn the reasonable flow fields. Additionally, the learned occlusion masks (4th column) also have the same shape as the target person, which indicates that our model can focus on the foreground region and select the most useful information from the source image.

Effect of Self-Training Part Replacement Strategy (STPR). As shown in Fig. 8(b), we observe that our full model could better preserve other regions than models without STPR. The 1-2 rows of Fig. 8(b) show that our full model could transfer the complex texture into the target person while preserving the pose of the source and face identity. On the other hand, the variant without STPR introduces substantial quality degradation in the face region and pose. Additionally, the 3rd row indicates that our refined strategy could provide a complete texture transfer. Table 3 demonstrates the quantitative comparison. Specifically, the full model with STPR shows obvious improvements in FID scores over all regions, for example, from 12.13 to 10.96 for ‘Face’ region, from 15.72 to 11.92 for ‘Tops’ region. This demonstrates that STPR could improve the realism of the transferred results. Moreover, the full model with STPR attains better Mask-LPIPS scores in most regions, which demonstrates the better preservation of the irrelevant source parts.

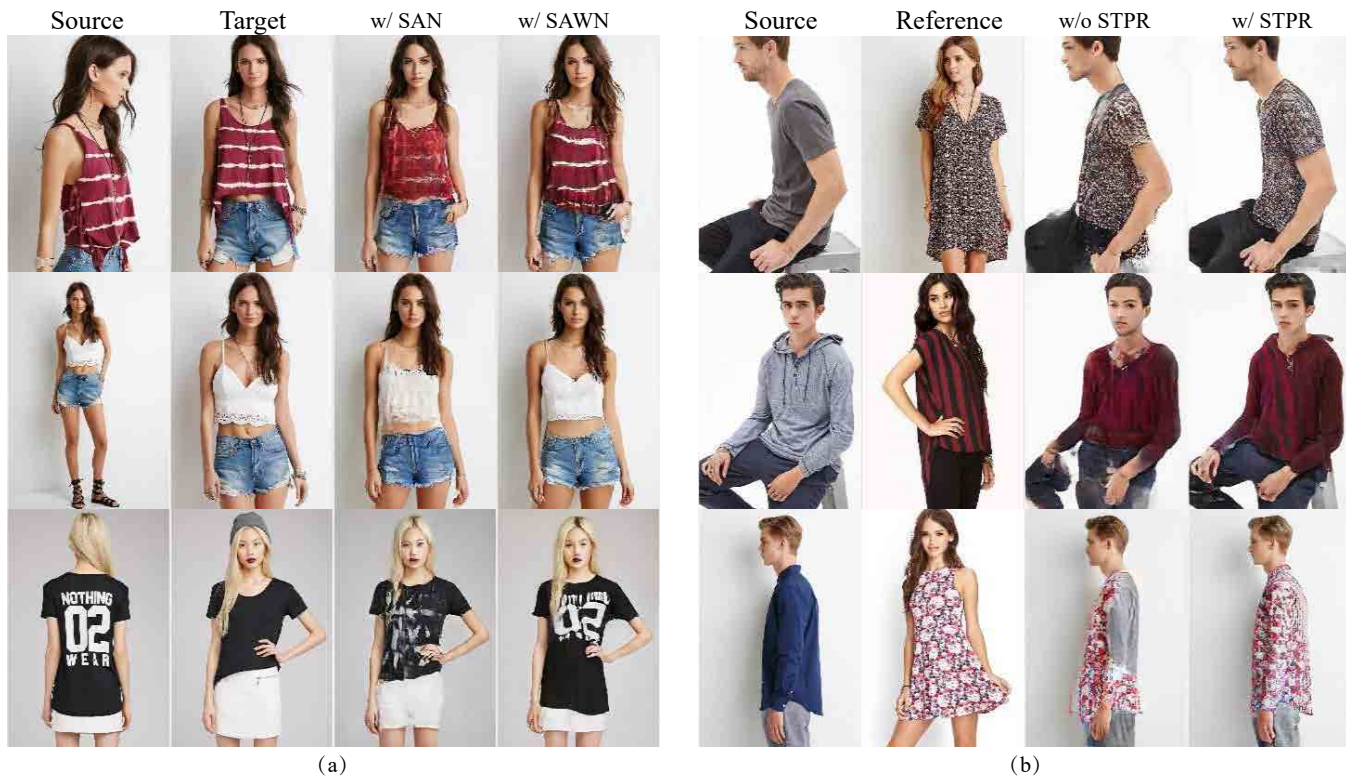


Fig. 8. (a) Comparison between our full model (with SAWN) and the variant (with SAN). SAN is the original spatially-adaptive instance normalization without a warped module. (b) Comparison between our full model with and without self-training part replacement strategy (STPR).

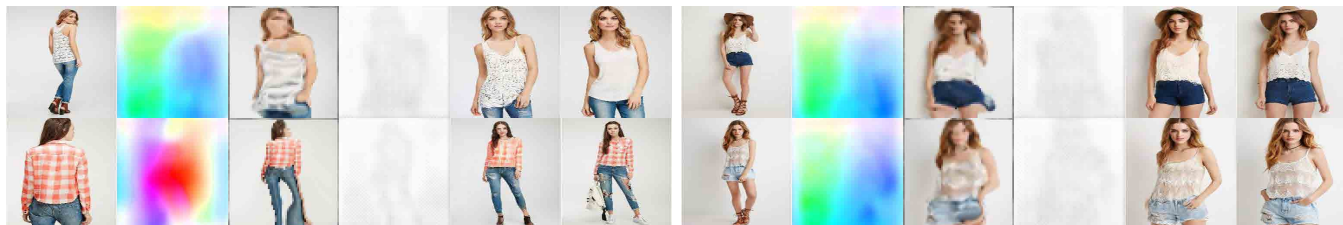


Fig. 9. Visualization of the learned flow field and occlusion mask. 1st column is the input person, and the next rows are the learned flow field, the warped results using the flow field for the input person, the occlusion mask, the generated results, the target person.

Table 4. Quantitative results between the full model (with SAWN) with our model with SAN instead of SAWN. SAN is the original spatially-adaptive instance normalization without a warped module.

Method	FID↓	LPIPS↓
w/ SAN	14.99	0.207
Our full model	11.54	0.196

6 CONCLUSIONS AND DISCUSSION

In this paper, we propose a novel spatially-adaptive warped normalization (SAWN) which aims to warp the modulation parameters to align the style and pose features. This block significantly improves the quality of the generated person image with complex poses and achieves a very realistic transfer of texture, especially the complex one. With extensive experiments, we validate the effectiveness and

superiority of the proposed model compared to the state-of-the-art methods. Although our method can achieve compelling results in many cases, the results are far from photorealistic in some cases, and there are still several limitations to be addressed in the future. **Inaccurate Segmentation Labels.** Recent methods [25, 35] and our method employ segmentation labels to disentangle the semantic parts of the person. However, the segmentation labels are generated by the parsing network. Thus they could be inaccurate, which causes the incorrect transfer in the texture-transfer task. To this end, we expect that training with ground truth segmentation could boost the performance significantly. Additionally, improved semantic segmentation could bring an additional performance boost at the test time.

Lack of Control over The Point of View. Our model, as well as other existing methods based on 2d keypoints, can synthesize person

images with the novel pose (extracted from the target image) but cannot generate the same person in a different view (given the new camera parameters). We plan to improve our method with control over view direction and camera parameters.

REFERENCES

- [1] Rameen Abdal, Yipeng Qin, and Peter Wonka. 2019. Image2stylegan: How to embed images into the stylegan latent space?. In *Proceedings of the IEEE/CVF International Conference on Computer Vision*. 4432–4441.
- [2] Rameen Abdal, Peihao Zhu, Niloy Mitra, and Peter Wonka. 2020. Styleflow: Attribute-conditioned exploration of stylegan-generated images using conditional continuous normalizing flows. *ACM Transactions on Graphics* (2020).
- [3] Thiemo Alldieck, Gerard Pons-Moll, Christian Theobalt, and Marcus Magnor. 2019. Tex2shape: Detailed full human body geometry from a single image. In *Proceedings of the IEEE/CVF International Conference on Computer Vision*. 2293–2303.
- [4] Vijay Badrinarayanan, Alex Kendall, and R. Cipolla. 2017. SegNet: A Deep Convolutional Encoder-Decoder Architecture for Image Segmentation. *IEEE Transactions on Pattern Analysis and Machine Intelligence* 39 (2017), 2481–2495.
- [5] G. Balakrishnan, Amy Zhao, Adrian V. Dalca, F. Durand, and J. Guttag. 2018. Synthesizing Images of Humans in Unseen Poses. *2018 IEEE/CVF Conference on Computer Vision and Pattern Recognition* (2018), 8340–8348.
- [6] Andrew Brock, Jeff Donahue, and Karen Simonyan. 2019. Large Scale GAN Training for High Fidelity Natural Image Synthesis. In *International Conference on Learning Representations*. <https://openreview.net/forum?id=B1xsqj09Fm>
- [7] Yunjeong Choi, Minje Choi, Munyoung Kim, Jung-Woo Ha, Sunghun Kim, and Jaegul Choo. 2018. Stargan: Unified generative adversarial networks for multi-domain image-to-image translation. In *Proceedings of the IEEE conference on computer vision and pattern recognition*. 8789–8797.
- [8] Yunjeong Choi, Youngjung Uh, Jaejun Yoo, and Jung-Woo Ha. 2020. StarGAN v2: Diverse Image Synthesis for Multiple Domains. In *Proceedings of the IEEE Conference on Computer Vision and Pattern Recognition*.
- [9] Vincent Dumoulin, Jonathon Shlens, and M. Kudlur. 2017. A Learned Representation For Artistic Style. *ArXiv abs/1610.07629* (2017).
- [10] Ian J Goodfellow, Jean Pouget-Abadie, Mehdi Mirza, Bing Xu, David Warde-Farley, Sherjil Ozair, Aaron Courville, and Yoshua Bengio. 2014. Generative adversarial networks. *arXiv preprint arXiv:1406.2661* (2014).
- [11] A. Grigorev, A. Sevastopolsky, Alexander Vakhitov, and V. Lempitsky. 2018. Coordinate-based Texture Inpainting for Pose-Guided Image Generation. *ArXiv abs/1811.11459* (2018).
- [12] Riza Alp Güler, Natalia Neverova, and Iasonas Kokkinos. 2018. Densepose: Dense human pose estimation in the wild. In *Proceedings of the IEEE conference on computer vision and pattern recognition*. 7297–7306.
- [13] Xintong Han, Zuxuan Wu, Zhe Wu, Ruichi Yu, and Larry S Davis. 2018. Viton: An image-based virtual try-on network. In *Proceedings of the IEEE conference on computer vision and pattern recognition*. 7543–7552.
- [14] Xintong Han, Zuxuan Wu, Zhe Wu, Ruichi Yu, and Larry S Davis. 2018. VITON: An Image-based Virtual Try-on Network. In *CVPR*.
- [15] Yu Han, Shuai Yang, Wenjing Wang, and Jiaying Liu. 2020. From Design Draft to Real Attire: Unaligned Fashion Image Translation. In *Proceedings of the 28th ACM International Conference on Multimedia*. 1533–1541.
- [16] Martin Heusel, Hubert Ramsauer, Thomas Unterthiner, Bernhard Nessler, and Sepp Hochreiter. 2017. Gans trained by a two time-scale update rule converge to a local nash equilibrium. In *NeurIPS*.
- [17] Siyu Huang, Haoyi Xiong, Zhi-Qi Cheng, Qingzhong Wang, Xingran Zhou, Bi-han Wen, Jun Huan, and Dejing Dou. 2020. Generating Person Images with Appearance-aware Pose Stylizer. In *IJCAI*.
- [18] Xun Huang and Serge Belongie. 2017. Arbitrary Style Transfer in Real-time with Adaptive Instance Normalization. In *ICCV*.
- [19] X. Huang and Serge J. Belongie. 2017. Arbitrary Style Transfer in Real-Time with Adaptive Instance Normalization. *2017 IEEE International Conference on Computer Vision (ICCV)* (2017), 1510–1519.
- [20] Xun Huang, Ming-Yu Liu, Serge Belongie, and Jan Kautz. 2018. Multimodal unsupervised image-to-image translation. In *Proceedings of the European conference on computer vision (ECCV)*. 172–189.
- [21] Xun Huang, Ming-Yu Liu, Serge Belongie, and Jan Kautz. 2018. Multimodal Unsupervised Image-to-image Translation. In *ECCV*.
- [22] Satoshi Iizuka, Edgar Simo-Serra, and Hiroshi Ishikawa. 2017. Globally and locally consistent image completion. *ACM Transactions on Graphics (ToG)* 36, 4 (2017), 1–14.
- [23] Sergey Ioffe and Christian Szegedy. 2015. Batch normalization: Accelerating deep network training by reducing internal covariate shift. In *International conference on machine learning*. PMLR, 448–456.
- [24] Thibaut Issenbuth, J. Mary, and Clément Calauzènes. 2020. Do Not Mask What You Do Not Need to Mask: a Parser-Free Virtual Try-On. *ArXiv abs/2007.02721* (2020).
- [25] Zhang Jinsong, Li Kun, Lai Yu-Kun, and Yang Jingyu. 2021. PISE: Person Image Synthesis and Editing with Decoupled GAN. In *Computer Vision and Pattern Recognition (CVPR)*.
- [26] Tero Karras, S. Laine, and Timo Aila. 2019. A Style-Based Generator Architecture for Generative Adversarial Networks. *2019 IEEE/CVF Conference on Computer Vision and Pattern Recognition (CVPR)* (2019), 4396–4405.
- [27] Tero Karras, Samuli Laine, Miika Aittala, Janne Hellsten, Jaakko Lehtinen, and Timo Aila. 2020. Analyzing and improving the image quality of stylegan. In *Proceedings of the IEEE/CVF Conference on Computer Vision and Pattern Recognition*. 8110–8119.
- [28] Diederik P Kingma and Jimmy Ba. 2015. Adam: A method for stochastic optimization. In *ICLR*.
- [29] Cheng-Han Lee, Ziwei Liu, Lingyun Wu, and Ping Luo. 2020. MaskGAN: Towards Diverse and Interactive Facial Image Manipulation. In *IEEE Conference on Computer Vision and Pattern Recognition (CVPR)*.
- [30] Yining Li, Chen Huang, and Chen Change Loy. 2019. Dense intrinsic appearance flow for human pose transfer. In *CVPR*.
- [31] Ziwei Liu, Ping Luo, Shi Qiu, Xiaogang Wang, and Xiaoou Tang. 2016. Deepfashion: Powering robust clothes recognition and retrieval with rich annotations. In *CVPR*.
- [32] Matthew Loper, Naureen Mahmood, Javier Romero, Gerard Pons-Moll, and Michael J. Black. 2015. SMPL: A Skinned Multi-Person Linear Model. *ACM Trans. Graphics (Proc. SIGGRAPH Asia)* 34, 6 (Oct. 2015), 248:1–248:16.
- [33] Liqian Ma, Xu Jia, Qianru Sun, Bernt Schiele, Tinne Tuytelaars, and Luc Van Gool. 2017. Pose guided person image generation. In *Advances in Neural Information Processing Systems*. 405–415.
- [34] Liqian Ma, Qianru Sun, Stamatios Georgoulis, Luc Van Gool, Bernt Schiele, and Mario Fritz. 2018. Disentangled person image generation. In *CVPR*.
- [35] Yifang Men, Yiming Mao, Yuning Jiang, Wei-Ying Ma, and Zhouhui Lian. 2020. Controllable Person Image Synthesis with Attribute-Decomposed GAN. In *Computer Vision and Pattern Recognition (CVPR), 2020 IEEE Conference on*.
- [36] Sachit Menon, Alexandru Damian, Shijia Hu, Nikhil Ravi, and Cynthia Rudin. 2020. PULSE: Self-supervised photo upsampling via latent space exploration of generative models. In *Proceedings of the IEEE/CVF Conference on Computer Vision and Pattern Recognition*. 2437–2445.
- [37] Natalia Neverova, Riza Alp Güler, and Iasonas Kokkinos. 2018. Dense pose transfer. In *Proceedings of the European conference on computer vision (ECCV)*. 123–138.
- [38] Taesung Park, Ming-Yu Liu, Ting-Chun Wang, and Jun-Yan Zhu. 2019. Semantic Image Synthesis with Spatially-Adaptive Normalization. In *Proceedings of the IEEE Conference on Computer Vision and Pattern Recognition*.
- [39] Taesung Park, Ming-Yu Liu, Ting-Chun Wang, and Jun-Yan Zhu. 2019. Semantic image synthesis with spatially-adaptive normalization. In *Proceedings of the IEEE/CVF Conference on Computer Vision and Pattern Recognition*. 2337–2346.
- [40] Adam Paszke, Sam Gross, Francisco Massa, Adam Lerer, James Bradbury, Gregory Chanan, Trevor Killeen, Zeming Lin, Natalia Gimelshein, Luca Antiga, et al. 2019. Pytorch: An imperative style, high-performance deep learning library. *arXiv preprint arXiv:1912.01703* (2019).
- [41] Tiziano Portenier, Qiyang Hu, Attila Szabo, Siavash Arjomand Bigdeli, Paolo Favaro, and Matthias Zwicker. 2018. Faceshop: Deep sketch-based face image editing. *ACM Transactions on Graphics* (2018).
- [42] Xuelin Qian, Yanwei Fu, Tao Xiang, Wenxuan Wang, Jie Qiu, Yang Wu, Yu-Gang Jiang, and Xiangyang Xue. 2018. Pose-normalized image generation for person re-identification. In *ECCV*.
- [43] Bin Ren, Hao Tang, Fanyang Meng, Runwei Ding, Ling Shao, Philip HS Torr, and Nicu Sebe. 2021. Cloth Interactive Transformer for Virtual Try-On. *arXiv preprint arXiv:2104.05519* (2021).
- [44] Yurui Ren, Xiaoming Yu, Junming Chen, Thomas H Li, and Ge Li. 2020. Deep Image Spatial Transformation for Person Image Generation. *CVPR* (2020).
- [45] Tim Salimans, Ian Goodfellow, Wojciech Zaremba, Vicki Cheung, Alec Radford, and Xi Chen. 2016. Improved techniques for training gans. In *NeurIPS*.
- [46] Kripasindhu Sarkar, Vladislav Golyanik, Lingjie Liu, and Christian Theobalt. 2021. Style and Pose Control for Image Synthesis of Humans from a Single Monocular View. *arXiv preprint arXiv:2102.11263* (2021).
- [47] Kripasindhu Sarkar, Dushyant Mehta, Weipeng Xu, Vladislav Golyanik, and Christian Theobalt. 2020. Neural Re-Rendering of Humans from a Single Image. In *European Conference on Computer Vision (ECCV)*.
- [48] Aliaksandr Siarohin, Enver Sangineto, Stéphane Lathuilière, and Nicu Sebe. 2018. Deformable gans for pose-based human image generation. In *CVPR*.
- [49] Zhentao Tan, Dongdong Chen, Qi Chu, Menglei Chai, Jing Liao, Mingming He, Lu Yuan, Gang Hua, and Nenghai Yu. 2021. Efficient Semantic Image Synthesis via Class-Adaptive Normalization. *IEEE Transactions on Pattern Analysis and Machine Intelligence* (2021).
- [50] Hao Tang, Song Bai, Philip HS Torr, and Nicu Sebe. 2020. Bipartite Graph Reasoning GANs for Person Image Generation. In *BMVC*.
- [51] Hao Tang, Song Bai, Li Zhang, Philip HS Torr, and Nicu Sebe. 2020. XingGAN for Person Image Generation. In *ECCV*.

- [52] Ondřej Texler, David Futschik, Michal Kučera, Ondřej Jamriška, Šárka Sochorová, Menglei Chai, Sergey Tulyakov, and Daniel Šykora. 2020. Interactive Video Stylization Using Few-Shot Patch-Based Training. *ACM Transactions on Graphics* 39, 4 (2020), 73.
- [53] Dmitry Ulyanov, Andrea Vedaldi, and Victor Lempitsky. 2016. Instance normalization: The missing ingredient for fast stylization. *arXiv preprint arXiv:1607.08022* (2016).
- [54] D. Ulyanov, A. Vedaldi, and V. Lempitsky. 2016. Instance Normalization: The Missing Ingredient for Fast Stylization. *ArXiv abs/1607.08022* (2016).
- [55] Bochao Wang, Huabin Zheng, Xiaodan Liang, Yimin Chen, and Liang Lin. 2018. Toward Characteristic-Preserving Image-based Virtual Try-On Network. In *Proceedings of the European Conference on Computer Vision (ECCV)*. 589–604.
- [56] Ting-Chun Wang, Ming-Yu Liu, Jun-Yan Zhu, Andrew Tao, Jan Kautz, and Bryan Catanzaro. 2018. High-Resolution Image Synthesis and Semantic Manipulation with Conditional GANs. In *Proceedings of the IEEE Conference on Computer Vision and Pattern Recognition*.
- [57] Xintao Wang, Ke Yu, Chao Dong, and Chen Change Loy. 2018. Recovering realistic texture in image super-resolution by deep spatial feature transform. In *The IEEE Conference on Computer Vision and Pattern Recognition (CVPR)*.
- [58] Zhou Wang, Alan C Bovik, Hamid R Sheikh, and Eero P Simoncelli. 2004. Image quality assessment: from error visibility to structural similarity. *IEEE TIP* 13, 4 (2004), 600–612.
- [59] Shih-En Wei, Jason Saragih, Tomas Simon, Adam W Harley, Stephen Lombardi, Michal Perdoch, Alexander Hypes, Dawei Wang, Hernan Badino, and Yaser Sheikh. 2019. Vr facial animation via multiview image translation. *ACM Transactions on Graphics (TOG)* 38, 4 (2019), 1–16.
- [60] Yuxin Wu and Kaiming He. 2018. Group normalization. In *Proceedings of the European conference on computer vision (ECCV)*. 3–19.
- [61] Han Yang, Ruimao Zhang, Xiaobao Guo, Wei Liu, Wangmeng Zuo, and Ping Luo. 2020. Towards Photo-Realistic Virtual Try-On by Adaptively Generating-Preserving Image Content. In *IEEE/CVF Conference on Computer Vision and Pattern Recognition (CVPR)*.
- [62] Ruiyun Yu, Xiaoqi Wang, and Xiaohui Xie. 2019. VTNFP: An Image-Based Virtual Try-On Network With Body and Clothing Feature Preservation. In *Proceedings of the IEEE/CVF International Conference on Computer Vision (ICCV)*.
- [63] Jichao Zhang, Yezhi Shu, Songhua Xu, Gongze Cao, Fan Zhong, Meng Liu, and Xueying Qin. 2018. Sparsely grouped multi-task generative adversarial networks for facial attribute manipulation. In *Proceedings of the 26th ACM international conference on Multimedia*. 392–401.
- [64] Richard Zhang, Phillip Isola, Alexei A Efros, Eli Shechtman, and Oliver Wang. 2018. The Unreasonable Effectiveness of Deep Features as a Perceptual Metric. In *CVPR*.
- [65] Dongdong Chen, Jing Liao, Qi Chu, Lu Yuan, Sergey Tulyakov, Zhentao Tan, Menglei Chai, and Nenghai Yu. 2020. MichiGAN: Multi-Input-Conditioned Hair Image Generation for Portrait Editing. *ACM Transactions on Graphics (TOG)* 39, 4 (2020), 1–13.
- [66] Yang Zhou, Xintong Han, Eli Shechtman, Jose Echevarria, Evangelos Kalogerakis, and Dingzeyu Li. 2020. MakelTalk: speaker-aware talking-head animation. *ACM Transactions on Graphics (TOG)* 39, 6 (2020), 1–15.
- [67] Jun-Yan Zhu, Taesung Park, Phillip Isola, and Alexei A Efros. 2017. Unpaired image-to-image translation using cycle-consistent adversarial networks. In *Proceedings of the IEEE international conference on computer vision*. 2223–2232.
- [68] Peihao Zhu, Rameen Abdal, Yipeng Qin, and Peter Wonka. 2020. SEAN: Image Synthesis With Semantic Region-Adaptive Normalization. In *IEEE/CVF Conference on Computer Vision and Pattern Recognition (CVPR)*.
- [69] Zhen Zhu, Tengpeng Huang, Baoguang Shi, Miao Yu, Bofei Wang, and Xiang Bai. 2019. Progressive pose attention transfer for person image generation. In *CVPR*.
- [70] Zhen Zhu, Zhi liang Xu, Ansheng You, and X. Bai. 2020. Semantically Multi-Modal Image Synthesis. *2020 IEEE/CVF Conference on Computer Vision and Pattern Recognition (CVPR)* (2020), 5466–5475.